BldC delays entry into development to produce a sustained period of vegetative growth in *Streptomyces venezuelae*

Matthew J. Bush[1,*], Govind Chandra[1], Mahmoud M. Al-Bassam[1,#], Kim C. Findlay[2] and Mark J. Buttner[1]

[1]*Department of Molecular Microbiology*, and [2]*Department of Cell and Developmental Biology, John Innes Centre, Norwich Research Park, Norwich NR4 7UH, UK*.

* To whom correspondence should be addressed. Tel: 44 (0) 1603 450757; Fax: 44 (0) 1603 450778; Email:matt.bush@jic.ac.uk

[#] Current address: Department of Paediatrics, Division of Host−Microbe Systems and Therapeutics, University of California San Diego, 9500 Gilman Drive, La Jolla, CA 92093, USA

KEYWORDS Morphological differentiation; sporulation; cell division; transcriptional regulation.

Word count Abstract: 234

Word count Importance Statement 150

Word count text (excluding references, footnotes and figure legends): 4606

ABSTRACT

Streptomycetes are filamentous bacteria that differentiate by producing spore-bearing reproductive structures called aerial hyphae. The transition from vegetative to reproductive growth is controlled by the *bld* (bald) loci, and mutations in *bld* genes prevent the formation of aerial hyphae, either by blocking entry into development (typically mutations in activators) or by inducing precocious sporulation in the vegetative mycelium (typically mutations in repressors). One of the *bld* genes, *bldC*, encodes a 68-residue DNA-binding protein related to the DNA-binding domain of MerR-family transcription factors. Recent work has shown that BldC binds DNA by a novel mechanism, but there is less insight into its impact on *Streptomyces* development. Here we used ChIP-seq coupled with RNA-seq to define the BldC regulon in the model species *Streptomyces venezuelae*, showing that BldC can function both as a repressor and as an activator of transcription. Using electron microscopy and time-lapse imaging, we show that *bldC* mutants are bald because they initiate development prematurely, bypassing the formation of aerial hyphae. This is consistent with the premature expression of BldC target genes encoding proteins with key roles in development (e.g. *whiD*, *whiI*, *sigF*), chromosome condensation and segregation (e.g. *smeA-sffA*, *hupS*), and sporulation-specific cell division (e.g. *dynAB*), suggesting that BldC-mediated repression is critical to maintain a sustained period of vegetative growth prior to sporulation. We discuss the possible significance of BldC as an evolutionary link between MerR family transcription factors and DNA architectural proteins.

IMPORTANCE

Understanding the mechanisms that drive bacterial morphogenesis depends on the dissection of the regulatory networks that underpin the cell biological processes involved. Recently, *Streptomyces venezuelae* has emerged as an attractive new model system for the study of morphological differentiation in *Streptomyces*. This has led to significant progress in identifying the genes controlled by the transcription factors that regulate aerial mycelium formation (Bld regulators) and sporulation (Whi regulators). Taking advantage of *S. venezuelae*, we used ChIP-seq coupled with RNA-seq to identify the genes directly under the control of BldC. Because *S. venezuelae* sporulates in liquid culture, the complete spore-to-spore life cycle can be examined using time-lapse microscopy, and we applied this technique to the *bldC* mutant. These combined approaches reveal BldC to be a member of an emerging class of Bld regulators that function principally to repress key sporulation genes, thereby extending vegetative growth and blocking the onset of morphological differentiation.

INTRODUCTION

The complex *Streptomyces* life cycle involves two distinct filamentous cell forms: the growing or vegetative hyphae and the reproductive or aerial hyphae, which differentiate into long chains of spores (1-6). Genetic studies identified the regulatory loci that control entry into development, which are called *bld* (bald) genes because null mutations in these loci prevent the formation of aerial hyphae. However, baldness can arise for two different reasons. The larger class of *bld* mutants, which define positive regulators, fail to initiate development, forming colonies of undifferentiated vegetative mycelium. In contrast, a smaller but growing class of *bld* mutants, which define negative regulators, enter development prematurely, inducing sporulation in the vegetative mycelium and bypassing the formation of aerial hyphae. Thus, macroscopically these two classes of mutants look similar, forming smooth colonies that lack the 'hairy' appearance of the wild type, but microscopically it is apparent that they arise for diametrically opposed reasons (5, 7-9).

BldC is a small, 68-residue protein with a winged Helix-Turn-Helix (wHTH) motif, related to those found in MerR-family proteins (10). The basic structure of classical MerR proteins is a dimer consisting of two identical subunits, each composed of an N-terminal wHTH DNA-binding domain, a C-terminal effector-recognition domain and an interconnecting linker region that consists of a long α-helix that interacts with the same helix in the other subunit, forming an antiparallel coiled-coil responsible for homodimerization. MerR proteins share significant sequence similarity only within their DNA-binding domains; as different family members bind different effectors, their C-terminal domains are variable and show little, if any, similarity to one another.

MerR transcription factors bind to palindromic DNA sequences as homodimers. However, unlike classical members of the MerR family, BldC has neither an effector domain nor the

dimerization helix, and BldC behaves as a monomer in free solution (11). As a consequence, how BldC might bind DNA remained unclear. To address this question, Schumacher et al. (11) carried out biochemical and structural studies to characterize the binding of *S. coelicolor* BldC to the promoters of two known target genes, *whiI* and *smeA*. These studies showed that BldC binds DNA in a completely different way to classical MerR regulators, instead involving asymmetric, cooperative, head-to-tail oligomerization on DNA direct repeats with concomitant pronounced DNA distortion (11). The number of direct repeats present in BldC-binding sites is variable, thus allowing cooperative, head-to-tail binding of additional BldC monomers. Since BldC-like proteins radiate throughout the bacteria, this study identified BldC as the founding member of a new structural family of transcription factors.

Although the work by Schumacher et al. (11) has provided a clear mechanistic understanding of how BldC binds DNA, there has been less insight into its biological role and impact on *Streptomyces* development. In part, this is because previous studies have focussed on the classical model species, *S. coelicolor*, which sporulates only on solid medium. Here we exploit the benefits of the new model species, *Streptomyces venezuelae*, which sporulates in liquid culture (12), to study the biological role of BldC. Using ChIP-seq coupled with RNA-seq, we identify the genes under BldC control and show that BldC can function both as a repressor and as an activator of transcription. We show that *bldC* mutants are bald because they enter development prematurely, bypassing the formation of aerial hyphae. This correlates with the premature expression of BldC target genes with key roles in development, chromosome condensation and segregation, and sporulation-specific cell division, suggesting that BldC-mediated repression is critical to maintain a sustained period of vegetative growth prior to sporulation.

RESULTS

Deletion of *bldC* causes premature initiation of development

We constructed an *S. venezuelae bldC* mutant by replacing the *bldC* coding region with an apramycin resistance (*apr*) cassette. The resulting mutant was bald, unable to produce the reproductive aerial hyphae that give mature wild-type *Streptomyces* colonies their characteristic fuzzy appearance (Fig. 1). However, scanning electron microscopy (SEM) of mature colonies of the *bldC* mutant showed that most of the biomass consisted of spores, rather than undifferentiated vegetative hyphae (Fig. 2). Comparison of the growth of the wild type and the *bldC* mutant on plates over time showed that after one day they looked similar (vegetative growth only) but after two days the wild type had produced aerial hyphae while the *bldC* mutant was still restricted to vegetative growth. After 3 days, the aerial hyphae of the wild type had differentiated into spores, and most of the biomass of the *bldC* mutant had also differentiated into spores, bypassing aerial mycelium formation. The *bldC* mutant also seemed to produce higher levels of extracellular matrix than the wild type (Fig. 2). The *bldC* mutant phenotype was fully complemented by introducing a single copy of the *bldC* gene under the control of its native promoter, expressed *in trans* from the ΦBT1 integration site (Figs. 1 and 2).

Using an established microfluidic system and methodology (12), we conducted fluorescence time-lapse microscopy to further study the developmental defects associated with deletion of *bldC*. As in previous studies (7, 12-13), we introduced an FtsZ-YPet translational fusion into the wild type, mutant and complemented mutant strains, allowing us to monitor each of the two distinct modes of cell division that occur in *Streptomyces*. In Fig. 3, the scattered single Z-rings mark the position of vegetative cross-walls, which do not constrict or give rise to cell-cell separation, but simply divide the vegetative hyphae into long, box-like compartments

(e.g. Figs. 3A + C, panel 2). In contrast, during reproductive growth, long ladders of regularly spaced Z-rings are synchronously deposited along sporogenic hyphae. These Z-rings mark the sites of sporulation septa, which do constrict, ultimately leading to the formation of chains of spores (e.g. Figs. 3A and C, panels 3 and 4). Time-lapse imaging of strains harbouring the FtsZ-YPet fusion showed that the duration of vegetative growth was shorter in the *bldC* mutant compared to the wild type and the complemented mutant (Fig. 3 and Movies S1 A/B, S2 A/B and S3 A/B). Noticeably, following germination, hyphal outgrowth in the *bldC* mutant was associated with an immediate increase in FtsZ-YPet expression, leading to the precocious formation of ladders of Z-rings (Fig. 3B and Movie S2A/B). However, although ladders of Z-rings were observed as early as 4 hours in the *bldC* mutant, mature spores were not observed in the corresponding DIC images until 21 hours, the same time that mature spores were seen in the wild type (Figs. 3A and B). Wild-type patterns of FtsZ expression and sporulation were restored in the complemented mutant (Fig. 3C and Movie S3A/B). From these data, we concluded that the overall role of BldC is to sustain vegetative growth and delay entry into development.

BldC levels are highest early in development

Using an anti-BldC polyclonal antibody, we monitored BldC levels in *S. venezuelae* during sporulation in liquid culture. Western blotting showed that BldC is abundant throughout the life cycle, but that BldC levels are highest early on, during vegetative growth (Fig. 4).

Defining the BldC regulon in *S. venezuelae*

Previously, ChIP-seq (or ChIP-chip) coupled with transcriptional profiling has enabled us to define the regulons of several key developmental regulators in *S. venezuelae* (14-17). Here, we employed the same approach, using an anti-BldC polyclonal antibody to identify the

promoters directly bound by BldC. We performed ChIP-seq at two distinct stages of vegetative growth when BldC was abundant: early vegetative growth (10 hr) and pre-sporulation (14 hr). This work revealed ~360 potential gene targets, the majority of which were bound by BldC at both time points (Table S1A). These targets include many genes encoding key transcriptional regulators of the *Streptomyces* developmental cascade (e.g. *bldM, whiB, wblA, whiD, whiH, whiI, sigF* and *bldC* itself), others encoding proteins involved in chromosome condensation and segregation during sporulation (e.g. *hupS, smeA-sffA*), and those directly involved in cell division during sporulation (e.g. *dynAB, ssgB*) (Fig. 5 and Table 1). Schumacher et al. (11) characterized the interaction of *S. coelicolor* BldC with the promoters of two of its previously known targets, *whiI* and the *smeA-ssfA* operon. *whiI* encodes an orphan response regulator that is essential for the later stages of sporulation, when it forms a functional heterodimer with a second orphan response regulator, BldM, enabling WhiI to bind to DNA and regulate the expression of ~40 sporulation genes (14). The *smeA-sffA* operon encodes a small membrane protein (SmeA) that recruits a DNA translocase (SffA) to sporulation septa (18). Deletion of *smeA-sffA* results in a defect in spore chromosome segregation and has pleiotropic effects on spore maturation (18).

Schumacher et al. (11) showed that BldC binds to DNA in a head-to-tail fashion at a variable number of direct repeats. So, for example, in the *whiI*-BldC structure, there are two direct repeats resulting in the head-to-tail oligomerisation of two BldC monomers, whereas in the *smeA*-BldC structure there are four direct repeats resulting in the head-to-tail oligomerisation of four BldC monomers. In line with this, our data show a broader BldC ChIP-seq peak at the *smeA* promoter compared to the *whiI* promoter (Fig. 5). Indeed, regions of BldC enrichment across the *S. venezuelae* genome were often noticeably broad. Approximately 60% of BldC targets were defined by narrow, *whiI*-like ChIP-seq peaks, but the remaining ~40% showed ChIP-seq peaks at least as broad as the peak observed at the *smeA* promoter (Fig. S1, Table

S2). The cooperative binding of BldC to DNA revealed by structural analysis (11) suggested that dimerization on DNA would be the minimum requirement for DNA binding and that extended multimerization would occur at target promoters carrying additional direct repeats. The BldC-DNA structures identified two major elements that define the specificity of BldC binding: a 4-bp AT-rich sequence with a C or G four-five nucleotides downstream. The consensus direct repeat is 5'-AATT(N_{3-4})(C/G)-3', but the BldC-*smeA* structure showed that conservation of even this degenerate consensus is not critical for BldC binding. In particular, for the AT-rich sequence, it is the narrowing of the minor groove caused by the AT-rich nature of that sequence that is important, rather than direct base reading by BldC (11). Because of this plasticity, it is not possible to predict BldC binding sites bioinformatically. Nevertheless, using this loose consensus as a guide, it seems likely that the BldC targets with narrow ChIP-seq peaks have two appropriately spaced direct repeat sequences, whereas BldC targets with broad ChIP-seq peaks, such as *smeA-sffA*, *cdgE* and *dynAB*, have more (Fig. S1).

BldC represses the transcription of a subset of target genes

whiI and the *smeA-sffA* operon were originally identified as BldC targets in *S. coelicolor* (11), but ChIP-seq analysis showed that they are also BldC targets in *S. venezuelae* (Fig. 5, Table 1). To assess the regulatory influence of BldC on the *whiI* and *smeA* promoters, we performed qRT-PCR using RNA isolated from wild-type *S. venezuelae* and the *bldC* mutant during vegetative growth (10 hr), when BldC is abundant in wild-type cells (Fig. 6). Under these conditions, expression of both *whiI* and *smeA* is significantly higher in the *bldC* mutant compared to the wild type. This suggests that BldC functions to repress the transcription of these developmental target genes during vegetative growth, consistent with the premature initiation of development seen in a *bldC* mutant. To gain a global view of the regulatory impact of BldC, we conducted RNA-seq to compare the transcriptomes of wild-type *S.*

185 *venezuelae* and the *bldC* mutant at 10 hr and 14 hr timepoints, when both strains were still
186 growing vegetatively (Table S1B). The RNA was prepared from the same cultures used to
187 make protein extracts for the BldC Western blotting shown in Fig. 4. In line with the qRT-
188 PCR data, *whiI* and *smeA* showed significant increases in expression in the *bldC* mutant
189 compared with the wild type. The *smeA* and *sffA* genes form an operon and, consistent with
190 this, both genes showed similar upregulation of expression at the 10 hr and 14 hr time points
191 (Table 1). In total, 156 of the genes we identified as BldC targets in ChIP-seq showed a
192 greater than 2-fold increase in expression in the *bldC* mutant (Table S1C and Fig. 7). These
193 included the key developmental genes *sigF*, *whiD* and *hupS*, which showed a greater than
194 two-fold increase in expression (logFC >1) in the *bldC* mutant, compared to the wild type at
195 both the 10 hr and 14 hr timepoints (Table 1). qRT-PCR confirmed the upregulation of *sigF*,
196 *whiD* and *hupS* expression in the *bldC* mutant relative to the wild type, as was observed for
197 *whiI* and *smeA* (Fig. 6).

198 Among the other BldC targets identified by ChIP-seq were a number of genes encoding
199 members of the Penicillin-Binding Protein (PBP) family, required for the synthesis of
200 peptidoglycan (19, 20). Our data indicates that the *vnz12970* and *vnz23255* genes, encoding
201 Class A high molecular mass (HMM) PBPs and the *vnz15130* gene, encoding a low
202 molecular mass (LMM) PBP, are all targets of BldC (Table 1). Expression of these PBP-
203 encoding genes is significantly upregulated in a *bldC* mutant during vegetative growth
204 compared to the wild type, showing that BldC functions to repress their transcription (Table
205 1).

206 Peptidoglycan synthesis is required to produce new wall material during cell elongation and
207 to produce septa during division (21). Most rod-shaped bacteria possess distinct gene-pairs to
208 control these two processes, a protein of the SEDS (shape, elongation, division, and
209 sporulation) family and its cognate class B PBP. In *E. coli*, the RodA-PBP2 and FtsW-FtsI

pairs control elongation and division respectively (22). In *S. venezuelae*, there are four equivalent SEDS-PBP pairs and our data indicate that one of these pairs, *vnz24690* and *vnz24685*, is under BldC control (Fig. 5 and Table 1). BldC binds upstream of this gene pair and both genes show >4-fold increase (logFC >2) in expression in the *bldC* mutant compared to the wild type.

In *Streptomyces*, the *ftsW-ftsI* SEDS-PBP gene pair is specifically required for cell division at sporulation septa (23). Both genes are found in the division and cell wall (*dcw*) gene cluster. This cluster encodes many proteins that play critical roles in hyphal polar growth, peptidoglycan biosynthesis and cell division, including DivIVA, SepF, SepG, FtsW and FtsZ. Closer inspection of the ChIP-seq data showed that BldC binds at multiple positions across the *dcw* cluster (Fig. 8), although these peaks all fall just below the significance threshold we applied ($p < E-04$) (Table S1A). The majority of genes within this cluster show a modest increase in expression (logFC 0.5-1.5) during vegetative growth in the *bldC* mutant relative to the wild type (Table S1D), suggesting that BldC functions to repress the transcription of genes within the *dcw* cluster during vegetative growth, in line with the premature initiation of cell division during sporulation that we observe in a *bldC* mutant.

Our data also indicate BldC-mediated repression of other genes with critical roles in cell division and sporulation such as the *dynAB* operon and *ssgB* (Fig. 5, Table 1). *dynA* and *dynB* encode two dynamin-like membrane-remodelling proteins that stabilize FtsZ rings during sporulation septation via protein-protein interactions with other divisome components including FtsZ, SepF, SepF2 and SsgB (13). In *S. coelicolor*, the actinomycete-specific proteins SsgA and SsgB positively control the spatial distribution of FtsZ rings during sporulation-specific cell division. SsgA binds and recruits SsgB, which in turn recruits FtsZ, determining the future sites of sporulation septation (24). Our data indicate that *ssgB* is a target of BldC-mediated repression (Table 1).

235

236 **BldC activates the transcription of a subset of target genes**

237 Strikingly, our RNA-seq data also reveal that large numbers of genes are significantly
238 downregulated in the *bldC* mutant during vegetative growth (Table S1B). Many of these
239 genes are not direct BldC targets but nevertheless encode proteins important for the formation
240 of an aerial mycelium, consistent with the bypassing of aerial hypha formation in the *bldC*
241 mutant (Table S1D). For example, for aerial hyphae to break surface tension and grow into
242 the air, they must be covered in an extremely hydrophobic sheath that is composed of two
243 families of developmentally regulated proteins, the chaplins and the rodlins. In wild-type *S.*
244 *venezuelae*, expression of the *chp* and *rdl* genes is activated at the onset of development, both
245 on plates and during submerged sporulation (14). In contrast, the *chp* and *rdl* genes were not
246 activated during submerged sporulation in the *bldC* mutant (Table S1E).

247

248 In addition to these indirect effects, 91 direct BldC target genes showed a greater than 2-fold
249 reduction in expression (logFC <-1) in the *bldC* mutant compared to the wild type during
250 vegetative growth, implying that BldC functions as an activator of these genes (Table S1E
251 and Fig. 7). Two of these BldC target genes encode the developmental regulators BldM and
252 WhiH, both of which showed significant down-regulation in the absence of *bldC* during
253 vegetative growth in the RNA-seq data (Table 1), a result confirmed by qRT-PCR (Fig. 6).
254 Therefore, BldC functions to activate the transcription of *bldM* and *whiH*, which contrasts
255 with its repression of other key developmental genes (e.g. *whiI*, *smeA*, *sigF*, *whiD* and *hupS*)
256 and the observed premature initiation of development in a *bldC* mutant. Our ChIP-seq data
257 coupled with our RNA-seq data also suggest that BldC binds and activates the transcription
258 of *ssgA* and *ssgR*, the latter encoding the sporulation-specific activator of *ssgA* (25) (Fig. 5
259 and Table 1).

Other noticeable targets of BldC-mediated activation include members of a family of highly conserved operons, known as the "conservons". Each conservon (*cvn*) consists of four or five genes encoding proteins that, based on biochemical studies of Cvn9, may collectively form complexes of proteins at the membrane with roles in signal transduction (26). Our RNA-seq data indicate that each of the seven conservons present on the *S. venezuelae* chromosome (*cvn1*, *cvn2*, *cvn3*, *cvn4*, *cvn5*, *cvn7* and *cvn9*) show a significant reduction in expression during vegetative growth in the *bldC* mutant compared to the wild type (Table S1D). Two (*cvn1* and *cvn4*) are direct targets of BldC, as determined by ChIP-seq (Fig. 5, Table 1). The promoter upstream of *cvn1* is also bound by WhiAB (17) and a *cvn1* mutant of *S. coelicolor* is impaired in aerial mycelium formation (27), collectively suggesting that Cvn1 (and perhaps other members of the conservon family) may play a significant but as yet undefined role in *Streptomyces* differentiation.

The importance of cyclic-di-GMP (c-di-GMP) in the control of *Streptomyces* differentiation became clear with the discovery that engineering high levels of this nucleotide second messenger blocks entry into development, resulting in a classic bald phenotype, whereas engineering low levels of ci-di-GMP causes precocious hypersporulation (5, 9). These phenotypes arise, at least in part, because the ability of the master repressor, BldD, to dimerize and repress a suite of sporulation genes during vegetative growth depends on binding to c-di-GMP (5, 9, 28, 29). c-di-GMP metabolism therefore plays a critical role in coordinating entry into reproductive growth. c-di-GMP is synthesized from two molecules of GTP by diguanylate cyclases (DGCs) and our ChIP-seq and RNA-seq data show that expression of *cdgE*, encoding a predicted DGC, is directly activated by BldC (Fig. 5 and

Table 1). *cdgE* is present in at least 90% of *Streptomyces* strains, suggesting the role of this DGC will be widely conserved in the genus (30).

Streptomyces sp. are noted producers of the terpene 2-methoisoborneol (2-MIB), one of the volatiles that give soil its characteristic earthy odour. Our RNA-seq data show that expression of the genes required for 2-MIB biosynthesis (*mibA-mibB*) was significantly reduced in the *bldC* mutant compared to the wild type (Table S1B). Unexpectedly, the *mibA-mibB* genes were found to form an operon with *eshA*. *eshA* encodes a putative cyclic nucleotide-binding protein of unclear function that is not required for the biosynthesis of 2-MIB (31-33). The effect of BldC on *mibAB* expression is direct. ChIP-seq analysis showed that BldC binds to the promoter of the *eshA-mibA-mibB* operon (Fig. 5 and Table 1) and that all three genes show a similar reduction in expression in the *bldC* mutant, indicating that BldC serves to activate transcription of the operon (Table 1).

DISCUSSION

Canonical *bld* mutations block entry into development and so the resulting colonies do not form aerial hyphae and spores. These mutations typically define positive regulators such as the response regulator BldM (16) or the sigma factor BldN (14). Although our data indicate that BldC can function as both an activator and a repressor, we have shown that *S. venezuelae bldC* mutants are bald because they enter development prematurely, bypassing the formation of aerial hyphae, and that this correlates with premature expression of a subset of BldC target genes with roles in *Streptomyces* differentiation. Thus, phenotypically, BldC functions as a repressor to sustain vegetative growth and delay entry into development. As such, BldC joins a growing class of Bld regulators known to function as a developmental “brake” (8).

BldD was the first Bld regulator of this alternative class to be clearly recognized. BldD sits at the top of the developmental cascade and represses a large regulon of ~170 sporulation genes during vegetative growth. BldD activity is controlled by the second messenger c-di-GMP, which mediates dimerization of two BldD protomers to generate a functional repressor. In this way, c-di-GMP signals through BldD to repress expression of the BldD regulon, extending vegetative growth and inhibiting entry into development (5, 9, 28, 29). Because a BldD-(c-di-GMP) complex represses the BldD regulon and not BldD alone, engineering the degradation of c-di-GMP *in vivo* also causes a precocious hypersporulation phenotype like that of a *bldD* null mutant (9).

More recently, *bldO* was identified as a second member of this emerging class of *bld* mutant (7, 8). In contrast to BldD and BldC, which both control large regulons, BldO functions to repress a single developmental gene, *whiB*. The precocious hypersporulation phenotype of the *bldO* mutant arises from premature expression of *whiB*, and in line with this, constitutive expression of *whiB* alone is sufficient to induce precocious hypersporulation in wild-type *S. venezuelae* (7). WhiA and WhiB act together to co-control the same set of promoters to initiate developmental cell division in *Streptomyces* (15, 17). WhiA is constitutively present throughout the life cycle, but it only binds to its target promoters at the onset of sporulation when WhiB is present (15, 17). This is because WhiA and WhiB function cooperatively and *in vivo* DNA binding by WhiA depends on WhiB, and *vice versa* (17). As a consequence, the regulation of *whiB* expression is key in controlling the switch between hyphal growth and sporulation. This critical role for WhiB is reflected in the extensive developmental regulation to which *whiB* transcription is subject, being directly repressed by BldC, BldD (28) and BldO (7), and directly activated by BldM (16).

BldC-family members radiate throughout the bacterial domain. Interestingly, some BldC orthologs are annotated as possible DNA resolvase/integrase-associated proteins, consistent with the structural similarity observed between BldC and Xis (11, 34). Xis is a DNA architectural protein that mediates the formation of a nucleoprotein complex required for the phage-encoded Int recombinase/integrase to catalyse the site-specific recombination event that leads to the excision of phage lambda from the *E. coli* chromosome. Like BldC, Xis binds to DNA in a head-tail fashion to generate a nucleoprotein filament, leading to distortion of the DNA (34). Thus, BldC may represent an evolutionary link between transcription factors of the MerR family and DNA architectural proteins (11).

There is an interesting analogy between the relationship of BldC to MerR and the relationship of Fis to NtrC. Fis is a 98-residue nucleoid-associated protein found in proteobacteria that is closely related to the DNA-binding domain of the much larger bacterial enhancer-binding protein NtrC (35-37). Like BldC, Fis prefers binding to A+T-rich DNA and its interaction with DNA is affected by the width of the minor groove (38). Fis can function in the cell as an architectural protein in the nucleoid, but it can also function as a transcription factor (39, 40). Like BldC, Fis exerts a global influence on the transcription profile of the cell and can have positive or negative effects on the activity of its target promoters (41). Fis does not bind a ligand and it is not known to be controlled by post-translational modification. Instead, its influence appears simply to reflect Fis protein concentration, which is high in early log phase but low at other growth stages. In the future, it will be interesting to determine if the activity of BldC is controlled post-translationally, or whether BldC function is more akin to that of nucleoid-associated proteins like Fis.

MATERIALS AND METHODS

Construction and complementation of an *S. venezuelae bldC* null mutant. Using 'Redirect' PCR targeting (42, 43), *bldC* mutants were generated in which the coding region was replaced with a single apramycin resistance (*apr*) cassette. A cosmid library that covers > 98% of the *S. venezuelae* genome (M.J. Bibb and M.J. Buttner, unpublished) is fully documented at http://strepdb.streptomyces.org.uk/. Cosmid 4O24 was introduced into *E. coli* BW25113 containing pIJ790 and the *bldC* gene (*sven3846*) was replaced with the *apr-oriT* cassette amplified from pIJ773 using the primer pairs bldCdis_F and bldCdis_R. The resulting disrupted cosmids were confirmed by restriction digestion and by PCR analysis using the flanking primers bldCcon_F and bldCcon_R, and introduced into *S. venezuelae* by conjugation (44). Null mutant derivatives, generated by double crossing over, were identified by their apramycin-resistant, kanamycin-sensitive and morphological phenotypes, and their chromosomal structures were confirmed by PCR analysis using the flanking primers bldCcon_F and bldCcon_R. A representative *bldC* null mutant was designated SV25. For complementation, *bldC* was amplified with the primers bldCcomp_F and bldCcomp_R, generating an 846bp fragment carrying the coding sequence and the *bldC* promoter, and cloned into HindIII-KpnI/Asp718 cut pIJ10770 to create pIJ10618. The plasmid was introduced into the *bldC* mutant by conjugation and fully complemented all aspects of the mutant phenotype.

Time-lapse imaging of *S. venezuelae*. Fluorescent time-lapse imaging was conducted essentially as described previously (7, 12, 13). Before imaging, fresh *S. venezuelae* spores for each of the strains imaged were first prepared by inoculating 30 ml cultures of MYM with 10 µl of the appropriate spore stock or 20 µl of the appropriate mycelial culture. Cells were cultured at 30 ºC and 250 rpm until fully differentiated (16-24 h for hypersporulating strains, otherwise 36-40 h). 1 ml of each culture was spun briefly to pellet mycelium, the supernatant

spores were diluted 1:50 in fresh MYM, and 50 µl was transferred to the cell loading well of a prepared B04A microfluidic plate (Merck-Millipore). The remaining culture was filter-sterilized to obtain spent MYM that was free of spores and mycelial fragments. The ONIX manifold was then sealed to the B04A plate before transferring to the environmental chamber, pre-incubated at 30 ºC. Spores were loaded onto the B04A plate, at 4 psi for 15 seconds using the ONIX microfluidic perfusion system. Fresh MYM medium was set to flow at 2 psi during the first 3 hours during germination, before the 2-psi flow of spent MYM medium for the remainder of the experiment. The system was left to equilibrate for 1 h prior to imaging.

Imaging was conducted using a Zeiss Axio Observer.Z1 widefield microscope equipped with a sCMOS camera (Hamamatsu Orca FLASH 4), a metal-halide lamp (HXP 120V), a hardware autofocus (Definitive Focus), a 96-well stage insert, an environmental chamber, a 100x 1.46 NA Oil DIC objective and the Zeiss 46 HE shift free (excitation500/25 nm, emission 535/30 nm) filter set. DIC images were captured with a 150 ms exposure time, YFP images were captured with a 100 ms exposure time. Images were taken every 30 min. In all experiments, multiple x/y positions were imaged for each strain and in each experiment. Representative images were transferred to the Fiji software package (http://fiji.sc/Fiji), manipulated and converted into the movie files presented here, as described previously (12).

ChIP-seq, RNA-seq, qRT-PCR, Western blotting and scanning electron microscopy See Supplemental Materials and Methods (Text S1).

FUNDING INFORMATION

This work was funded by BBSRC grant BB/H006125/1 (to M.J.B.) and by BBSRC Institute Strategic Programme Grant BB/J004561/1 to the John Innes Centre. The funders had no role in study design, data collection and interpretation, or the decision to submit the work for publication.

ACKNOWLEDGEMENTS

We are grateful to Ray Dixon and Charlie Dorman for helpful discussion, and to Genewiz for expert handling of the ChIP and RNA samples.

REFERENCES

1. Flärdh K, Buttner MJ. 2009. *Streptomyces* morphogenetics: dissecting differentiation in a filamentous bacterium. Nat Rev Microbiol 7:36-49.
2. McCormick JR, Flärdh K. 2012. Signals and regulators that govern *Streptomyces* development. FEMS Microbiol Rev 36:206-231.
3. McCormick JR. 2009. Cell division is dispensable but not irrelevant in *Streptomyces*. Curr Opin Microbiol 12:689-698.
4. Jakimowicz D, and van Wezel GP. 2012. Cell division and DNA segregation in *Streptomyces*: how to build a septum in the middle of nowhere? Mol Microbiol 85:393-404.
5. Bush MJ, Tschowri N, Schlimpert S, Flärdh K, Buttner MJ. 2015. c-di-GMP signaling and the regulation of developmental transitions in *Streptomyces*. Nat Rev Microbiol 13:749-760.
6. Chater KF. 2016. Recent advances in understanding *Streptomyces*. F1000Res 5:2795.
7. Bush MJ, Chandra G, Findlay KC, Buttner MJ. 2017. Multi-layered inhibition of *Streptomyces* development: BldO is a dedicated repressor of whiB. Mol. Microbiol. 104:700-711.
8. Flärdh K, McCormick JR. 2017. The *Streptomyces* O-B one connection: a force within layered repression of a key developmental decision. Mol. Microbiol 104:695-699.
9. Tschowri N, Schumacher MA, Schlimpert S, Chinnam NB, Findlay KC, Brennan RG, Buttner MJ. 2014. Tetrameric c-di-GMP mediates effective transcription factor dimerization to control *Streptomyces* development. Cell 158:1136-1147.
10. Hunt AC, Servin-Gonzalez L, Kelemen GH, Buttner MJ. 2005. The bldC developmental locus of *Streptomyces coelicolor* encodes a member of a family of small DNA-binding proteins related to the DNA-binding domains of the MerR family. J Bacteriol 187:716-

728.

11. Schumacher MA, den Hengst CD, Bush MJ, Le TB, Tran NT, Chandra G, Zeng W, Travis B, Brennan RG, Buttner MJ. 2018. The MerR-like protein BldC binds DNA direct repeats as cooperative multimers to regulate Streptomyces development. Nature Commun. 9:1139.

12. Schlimpert S, Flärdh K, Buttner, MJ. 2016. Fluorescence time-lapse imaging of the complete *Streptomyces* life cycle using a microfluidic device. J Vis Exp 108:e53863.

13. Schlimpert S, Wasserstrom S, Chandra G, Bibb MJ, Findlay KC, Flärdh K, Buttner MJ. 2017. Two dynamin-like proteins stabilize FtsZ rings during *Streptomyces* sporulation. Proc Natl Acad Sci U S A 114:E6176-E6183.

14. Bibb MJ, Domonkos A, Chandra G, Buttner MJ. 2012. Expression of the chaplin and rodlin hydrophobic sheath proteins in *Streptomyces venezuelae* is controlled by σ^{BldN} and a cognate anti-sigma factor, RsbN. Mol. Microbiol. 84:1033–1049.

15. Bush MJ, Bibb MJ, Chandra G, Findlay KC, Buttner MJ. 2013. Genes required for aerial growth, cell division, and chromosome segregation are targets of WhiA before sporulation in *Streptomyces venezuelae*. mBio 4:e00684-13.

16. Al-Bassam MM, Bibb MJ, Bush MJ, Chandra G, Buttner MJ. 2014. Response regulator heterodimer formation controls a key stage in *Streptomyces* development. PLoS Genet 10:e1004554.

17. Bush MJ, Chandra G, Bibb MJ, Findlay KC, Buttner MJ. 2016. Genome-wide chromatin immunoprecipitation sequencing analysis shows that WhiB is a transcription factor that co-controls its regulon with WhiA to initiate developmental cell division in *Streptomyces*. mBio 7:e00523-16.

18. Ausmees N, Wahlstedt H, Bagchi S, Elliot MA, Buttner MJ, Flärdh K. 2007. SmeA, a small membrane protein with multiple functions in *Streptomyces* sporulation including targeting of a SpoIIIE/FtsK-like protein to cell division septa. Mol Microbiol 65:1458-1473.

19. Macheboeuf P, Contreras-Martel C, Job V, Dideberg O, Dessen A. 2006. Penicillin binding proteins: key players in bacterial cell cycle and drug resistance processes. FEMS Microbiol. Rev. 30:673-691.

20. Sauvage E, Kerff F, Terrak M, Ayala JA, Charlier P. 2008. The penicillin□binding proteins: structure and role in peptidoglycan biosynthesis. FEMS Microbiol. Rev. 32:234-258.

21. Typas A, Banzhaf M, Gross CA, Vollmer W. 2011. From the regulation of peptidoglycan synthesis to bacterial growth and morphology. Nat Rev Microbiol. 10:123-36.

22. Mercer KL, Weiss DS. 2002. The *Escherichia coli* cell division protein FtsW is required to recruit its cognate transpeptidase, FtsI (PBP3), to the division site. J Bacteriol. 184:904-12.

23. Mistry BV, Del Sol R, Wright C, Findlay K, Dyson P. 2008. FtsW is a dispensable cell division protein required for Z-ring stabilization during sporulation septation in *Streptomyces coelicolor*. J Bacteriol. 190:5555-66.

24. Willemse J, Borst JW, de Waal E, Bisseling T, van Wezel GP 2011. Positive control of cell division: FtsZ is recruited by SsgB during sporulation of *Streptomyces*. Genes Dev 25:89–99.

25. Traag BA, Kelemen GH, Van Wezel GP. 2004. Transcription of the sporulation gene *ssgA* is activated by the IclR-type regulator SsgR in a *whi*-independent manner in *Streptomyces coelicolor* A3(2). Mol Microbiol. 53:985-1000.

488 26. Komatsu M, Takano H, Hiratsuka T, Ishigaki Y, Shimada K, Beppu T, Ueda K. 2006.
489 Proteins encoded by the conservon of *Streptomyces coelicolor* A3(2) comprise a
490 membrane-associated heterocomplex that resembles eukaryotic G protein-coupled
491 regulatory system. Mol Microbiol 62:1534-46.
492 27. Takano H, Hashimoto K, Yamamoto Y, Beppu T, Ueda K. 2011. Pleiotropic effect of a
493 null mutation in the *cvn1* conservon of *Streptomyces coelicolor* A3(2). Gene 477:12-8.
494 28. den Hengst CD, Tran NT, Bibb MJ, Chandra C, Leskiw BK, Buttner MJ. 2010. Genes
495 essential for morphological development and antibiotic production in *Streptomyces*
496 *coelicolor* are targets of BldD during vegetative growth. Mol Microbiol 78:361-379.
497 29. Schumacher MA, Zeng W, Findlay KC, Buttner MJ, Brennan RG, Tschowri N. 2017. The
498 *Streptomyces* master regulator BldD binds c-di-GMP sequentially to create a functional
499 $BldD_2$-$(c\text{-}di\text{-}GMP)_4$ complex. Nucleic Acids Res 45:6923-6933.
500 30. Al-Bassam MM, Haist J, Neumann SA, Lindenberg S, Tschowri N. 2018. Expression
501 patterns, genomic conservation and input into developmental regulation of the
502 GGDEF/EAL/HD-GYP domain proteins in *Streptomyces*. Front Microbiol 9:2524.
503 31. Saito N, Matsubara K, Watanabe M, Kato F, Ochi K. 2003. Genetic and biochemical
504 characterization of EshA, a protein that forms large multimers and affects developmental
505 processes in *Streptomyces griseus*. J Biol Chem 278:5902-5911.
506 32. Komatsu M, Tsuda M, Omura S, Oikawa H, Ikeda H. 2008. Identification and functional
507 analysis of genes controlling biosynthesis of 2-methylisoborneol. Proc Natl Acad Sci U S
508 A 105:7422-7.
509 33. Wang CM, Cane DE. 2008. Biochemistry and molecular genetics of the biosynthesis of
510 the earthy odorant methylisoborneol in *Streptomyces coelicolor*. J Am Chem Soc.
511 130:8908-9.

512 34. Abbani MA, Papagiannis CV, Sam MD, Cascio D, Johnson RC, Clubb RT. 2007.
513 Structure of the cooperative Xis-DNA complex reveals a micronucleoprotein filament
514 that regulates phage lambda intasome assembly. Proc Natl Acad Sci U S A 104:2109-14.
515 35. Morett E, Bork P. 1998. Evolution of new protein function: Recombinational enhancer
516 FIS originated by horizontal gene transfer from the transcriptional regulator NtrC. FEBS
517 Letters 433:108-112.
518 36. Kostrewa D, Granzin J, Koch C, Choe HW, Raghunathan S, Wolf W, Labahn J,
519 Kahmann R, Saenger W. 1991. Three-dimensional structure of the *E. coli* DNA-binding
520 protein FIS. Nature 349:178–180.
521 37. Pelton JG, Kustu S, Wemmer DE. 1999. Solution structure of the DNA-binding domain
522 of NtrC with three alanine substitutions. J Mol Biol 292:1095-110.
523 38. Stella S, Cascio D, Johnson RC. 2010. The shape of the DNA minor groove directs
524 binding by the DNA-bending protein Fis. Genes Dev 24:814–826.
525 39. Dame RT. 2005. The role of nucleoid-associated proteins in the organization and
526 compaction of bacterial chromatin. Mol Microbiol 56:858-70.
527 40. Dorman CJ. 2014. Function of nucleoid-associated proteins in chromosome structuring
528 and transcriptional regulation. J Mol Microbiol Biotechnol. 24:316-31.
529 41. Kahramanoglou C, Seshasayee AS, Prieto AI, Ibberson D, Schmidt S, Zimmermann J,
530 Benes V, Fraser GM, Luscombe NM. 2011. Direct and indirect effects of H-NS and Fis
531 on global gene expression control in *Escherichia coli*. Nucleic Acids Res 39:2073–2091.
532 42. Gust B, Challis GL, Fowler K, Kieser T, Chater KF. 2003 PCR-targeted *Streptomyces*
533 gene replacement identifies a protein domain needed for biosynthesis of the sesquiterpene
534 soil odor geosmin. Proc Natl Acad Sci USA 100:1541-1546.

535 43. Gust B, Chandra G, Jakimowicz D, Yuqing T, Bruton C, Chater KF. 2004. Lambda red-
536 mediated genetic manipulation of antibiotic-producing *Streptomyces*. Adv Appl
537 Microbiol 54: 107-128.
538 44. Kieser T, Bibb MJ, Buttner MJ, Chater KF, Hopwood DA. 2000. *Practical Streptomyces*
539 *genetics*. The John Innes Foundation, Norwich, United Kingdom.
540

541 **FIGURE LEGENDS**

542 **FIG 1.** BldC is required for the formation of aerial mycelium. Wild-type *S.venezuelae*, the
543 *bldC* mutant, the *bldC* mutant carrying the empty vector, and the complemented *bldC* mutant,
544 photographed after four days of growth on MYM solid medium.
545

546 **FIG 2.** Deletion of *bldC* causes premature initiation of development on solid medium.
547 Scanning electron micrographs showing the phenotypes of the *bldC* mutant and the wild type
548 after one, two and three days of growth on MYM solid medium. The phenotype of the
549 complemented *bldC* mutant is also shown after 3 days of growth on MYM solid medium.
550

551 **FIG 3.** Deletion of *bldC* causes premature initiation of development in liquid medium. Time-
552 lapse images (4, 7, 12 and 21 h post-inoculation) of (A) wild-type *S. venezuelae*, (B) the *bldC*
553 mutant, and (C) the complemented *bldC* mutant, grown in liquid MYM medium in the
554 microfluidic system. All three strains carry the same FtsZ-YPet translational fusion expressed
555 from the native ftsZ promoter, and both the DIC (upper) and fluorescence (lower) images are
556 shown. Scale Bar = 10μm. For the corresponding movies, please see Supporting Information
557 Movies S1A/B, S2A/B and S3 A/B.

558

559 **FIG 4.** Automated Western blot analysis of BldC levels during submerged sporulation in
560 MYM liquid medium. Equal amounts (1 µg) of total protein were loaded for each sample and
561 BldC was detected with a polyclonal antibody using the quantitative 'Wes' capillary
562 electrophoresis and blotting system (ProteinSimple – San Jose, CA). The *S. venezuelae bldC*
563 mutant was used as a negative control. (A) quantitation of BldC levels (area under each peak;
564 arbitrary units). (B) virtual Western blot. All experimental samples were analysed in triplicate
565 and the mean value and its Standard Error are shown for each sample. Each time point is
566 indicated in hours, along with its relation to the developmental stage (V = vegetative growth;
567 F = fragmentation; S = sporulation), as determined by microscopy. Cultures used to analyse
568 BldC levels were identical to those used to prepare RNA prior to qRT-PCR analysis (Fig. 6).

569

570 **FIG 5.** BldC ChIP-seq in *S. venezuelae*. ChIP traces are shown for 12 selected BldC target
571 genes/operons: *eshA-mibAB*, *wblA*, *ssgR-ssgA*, *dynAB*, *smeA-sffA*, *vnz23255*, *sigI*, *vnz24690-*
572 *24685*, *whiI*, *cvnA4-D4*, *cvnA1-D1* and *cdgE*. Color-coding of the ChIP samples is as follows:
573 *S. venezuelae* wild type 10 hr (WT 10 hr, red), *S. venezuelae* wild type 10hr (WT 14 hr,
574 green) and Δ*bldC* mutant 14 hr (Δ*bldC*, black). Plots span approximately 5 kb of DNA
575 sequence. Genes running left to right are shown in green, and genes running right to left are
576 shown in red. The black arrow indicates the gene of interest subject to BldC regulation.

577

578 **FIG 6.** qRT-PCR data showing mRNA abundance for the BldC target genes *whiI*, *smeA*,
579 *sigF*, *whiD*, *hupS*, *whiH* and *bldM* in the wild type (white bars) and the *bldC* mutant (black
580 bars). Strains were grown in MYM liquid medium. Expression values were calculated
581 relative to the accumulation of the constitutively expressed *hrdB* reference mRNA and
582 normalized to the wild type value at 10 h.

583

584 **FIG 7.** Volcano plots of the RNA-seq data at the 10 hr (left panel) and 14 hr (right panel)
585 time points with significance ($-\log_{10}$ P-value) plotted against differential expression (log fold
586 change). The thresholds for significant differential expression (>1 or <-1 log fold change) are
587 indicated via vertical dashed lines. Genes with log fold change >1/<-1 show at least a two-
588 fold increase/decrease in expression in the Δ*bldC* mutant relative to the wild type. Genes that
589 are BldC ChIP-seq targets in *S. venezuelae* are indicated by red dots.

590

591 **FIG 8.** BldC binds at multiple positions across the *dcw* operon. The genes found in the *dcw*
592 cluster are annotated. Color-coding of the ChIP samples is as follows: *S. venezuelae* wild type
593 10 hr (WT 10 hr, red), *S. venezuelae* wild type 10 hr (WT 14 hr, green) and Δ*bldC* mutant 14
594 hr (Δ*bldC*, black). Genes running left to right are shown in green, and genes running right to
595 left are shown in red. The black arrows indicate BldC binding sites identified in this analysis.

596

597 **Table 1.** Selected BldC ChIP-seq targets. Listed is the minimum p-value for the ChiP-seq
598 peak, the gene and the gene product. For each target, the RNA-seq data, showing the relative
599 expression values (logFC) for the Δ*bldC* mutant compared to the wild type at the 10 hr and
600 14 hr time points is also listed. Significant increases in relative expression (>1) are indicated
601 in red. Significant decreases in relative expression (<-1) are indicated in yellow. Where BldC
602 binding is likely to exert control over multiple genes in a single operon, the data for these
603 genes is also listed.

604

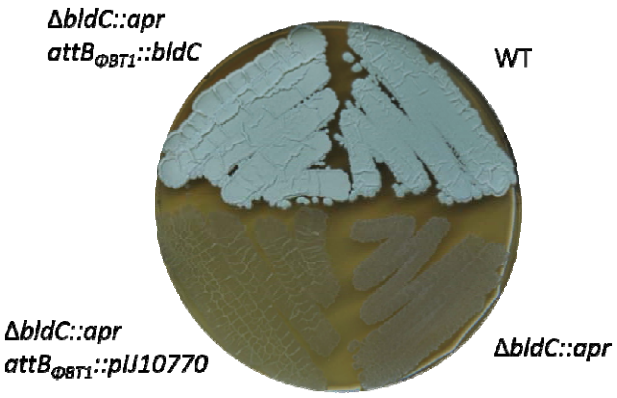

605 **FIG 1.**

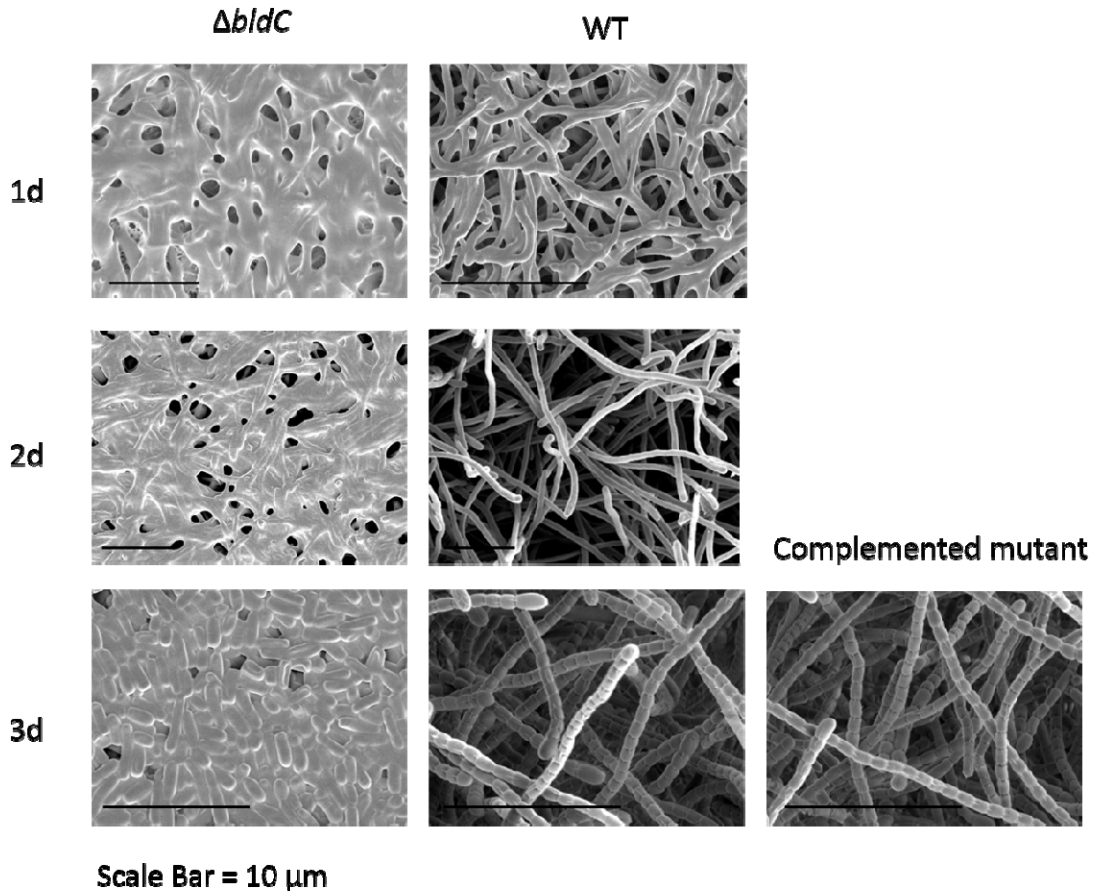

606

607 **FIG 2.**

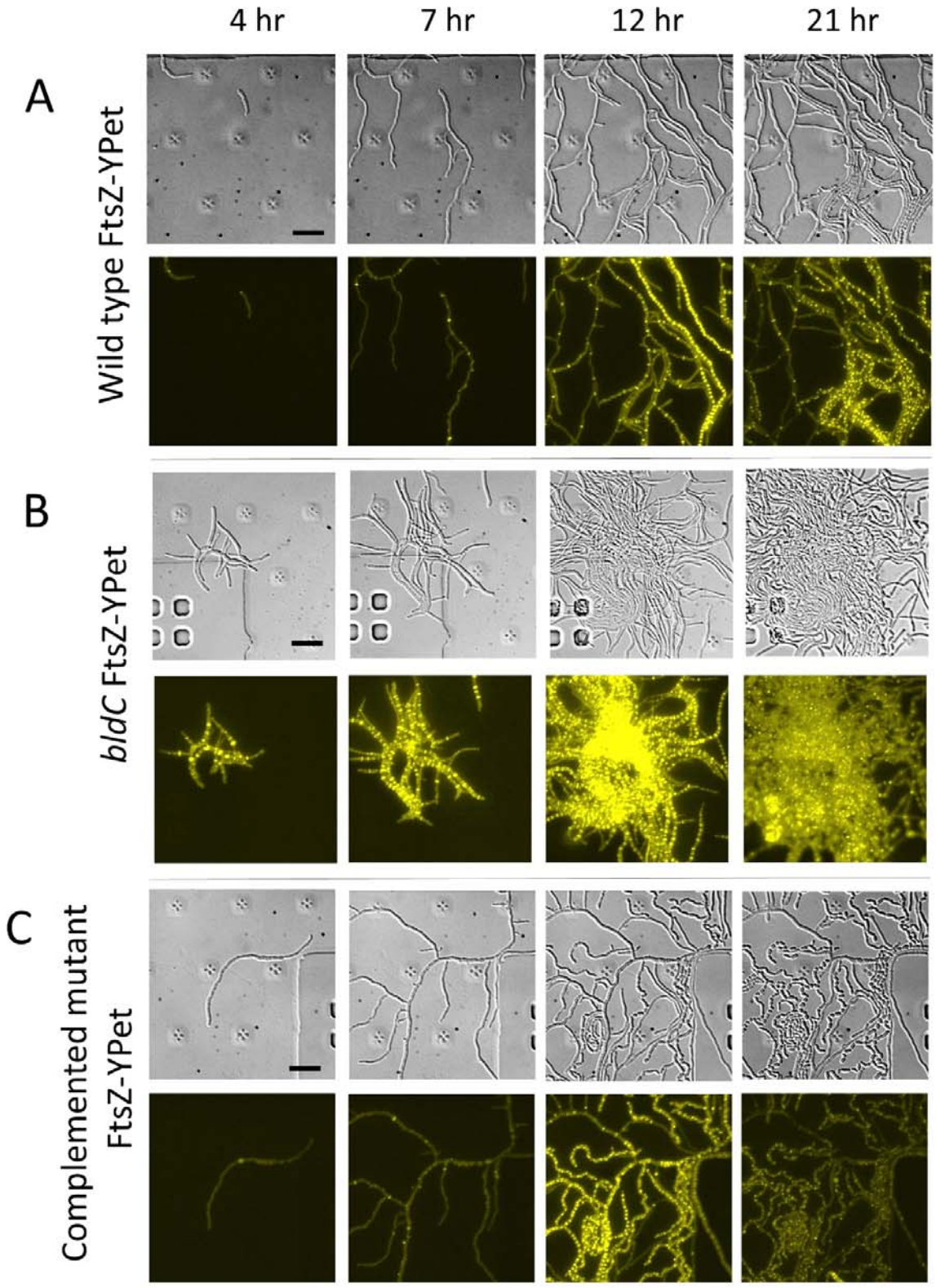

FIG 3.

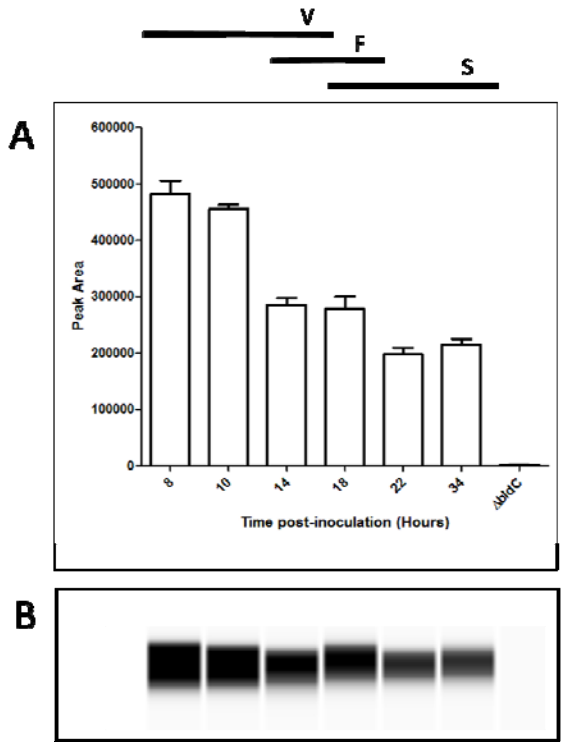

608 **FIG 4.**

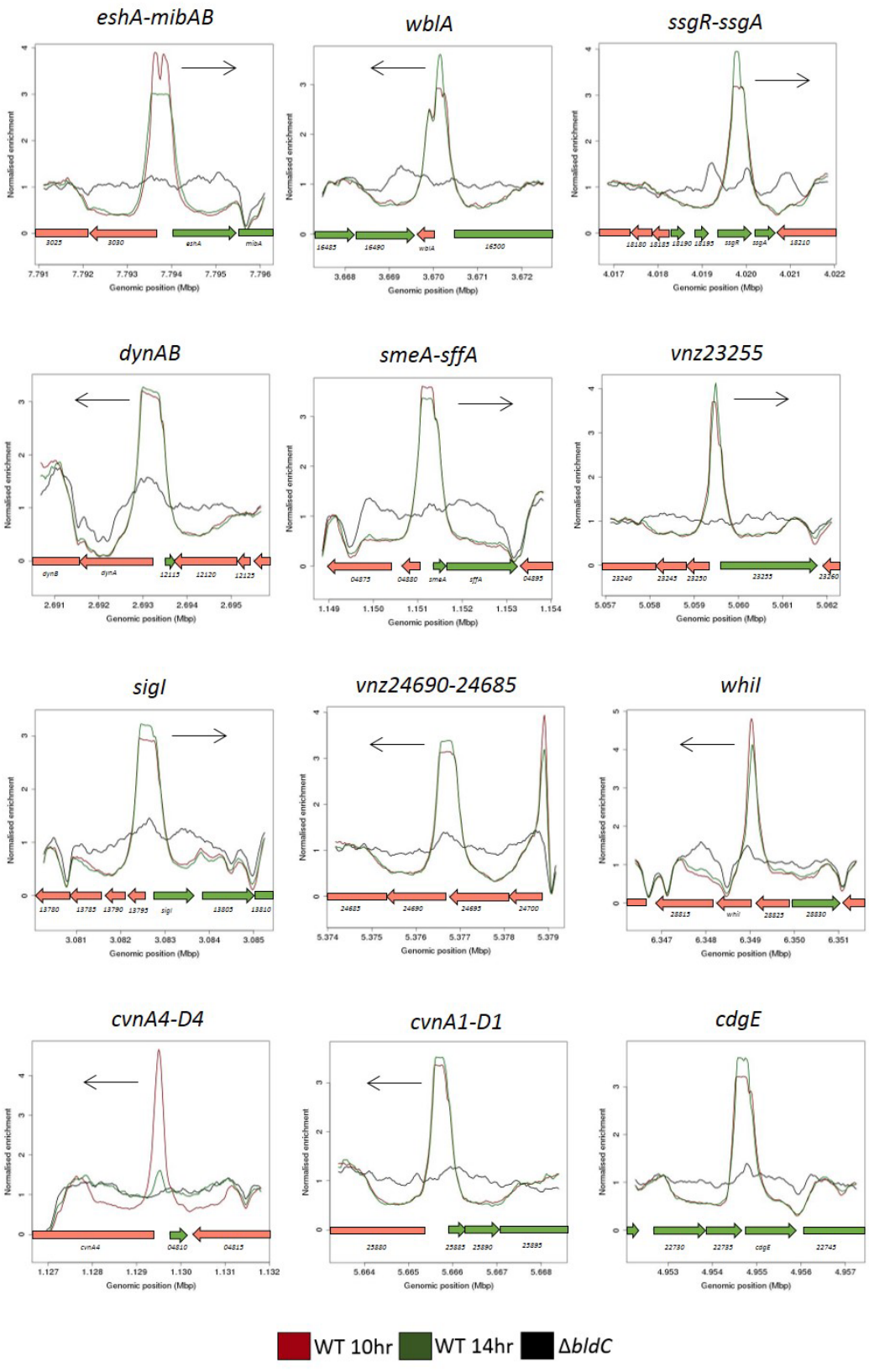

FIG 5.

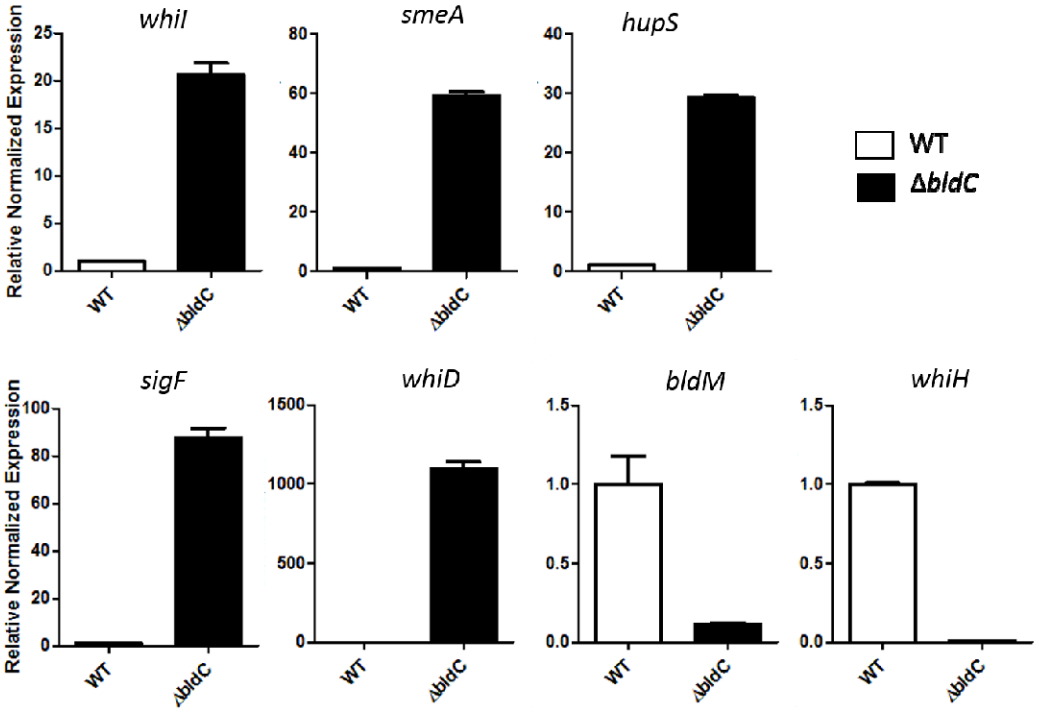

609 **FIG 6.**

610

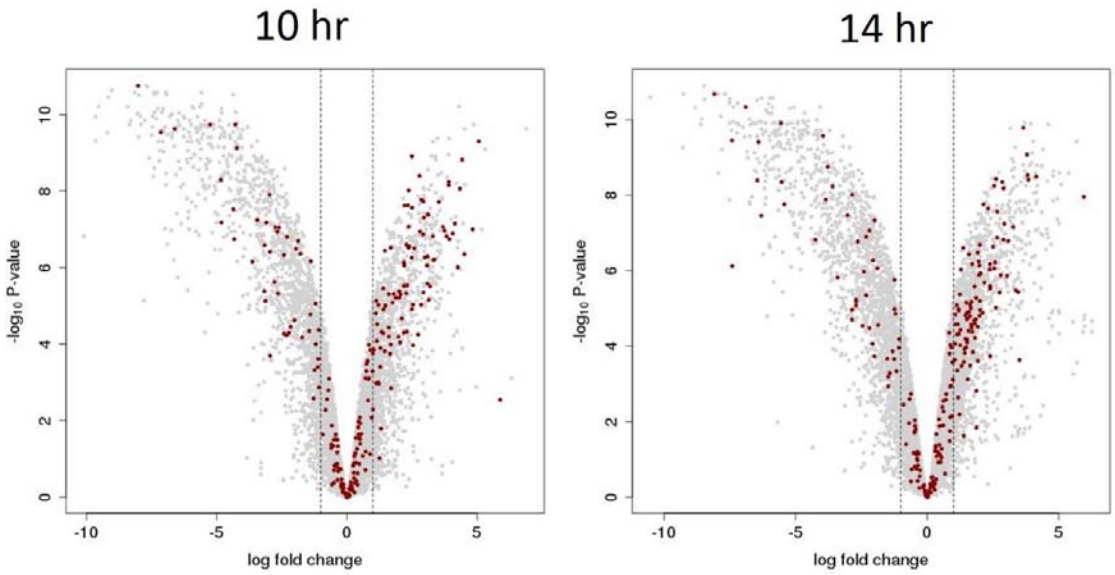

611 **FIG 7.**

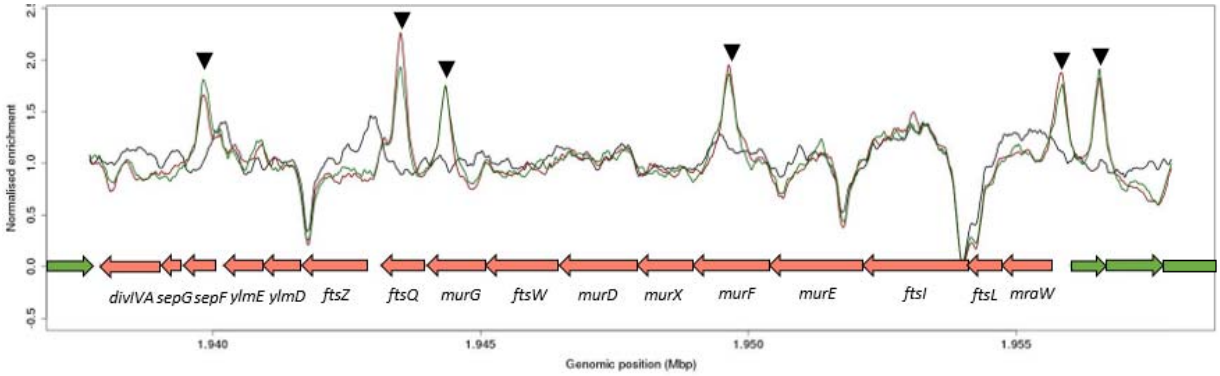

612

FIG 8.

613

min apv	Gene	Product	LogFC 10hr	LogFC 14hr
2.42E-10	vnz_18945	BldC	-	-
3.03E-18	vnz_35035	EshA	-8.1457	-5.3406
	vnz_35040	MibA	-4.8905	-2.8033
	vnz_35045	MibB	-6.4229	-5.1941
3.19E-17	vnz_16495	WblA	-4.3602	-5.5303
1.4E-06	vnz_27205	WhiH	-4.2208	-3.7707
1.33E-07	vnz_22005	BldM	-2.6717	-3.0249
5.39E-22	vnz_18205	SsgA	-1.8093	-0.5592
	vnz_18200	SsgR	-2.2995	-2.3179
4.48E-32	vnz_04805	CvnA4	-0.1815	-2.1394
	vnz_04800	CvnB4	0.0016	-2.6155
	vnz_04795	CvnC4	0.1926	-2.5418
	vnz_04790	CvnD4	-0.1034	-2.7909
3.37E-15	vnz_25880	CvnA1	0.0094	-1.1536
	vnz_25875	CvnB1	-0.0808	-1.5193
	vnz_25870	CvnC1	-0.1607	-2.2575
	vnz_25865	CvnD1	-0.0979	-2.2674
1.33E-07	vnz_22000	WhiD	6.8916	2.4359
1.33E-15	vnz_18620	SigF	4.4232	3.8513
2.52E-07	vnz_12110	DynA	3.0967	2.3950
	vnz_12105	DynB	3.1842	2.1040
1.23E-12	vnz_04885	SmeA	2.7343	0.1379
	vnz_04890	SffA	2.7046	0.3368
2.33E-12	vnz_05545	SsgB	2.5471	0.7373
4.06E-09	vnz_13800	SigI	2.5392	2.7563
1.48E-09	vnz_24690	FtsW-like	2.4867	1.8583
	vnz_24685	penicillin-binding protein	2.1361	2.0431
2.5E-15	vnz_22740	CdgE	2.2747	2.0130
1.87E-27	vnz_28820	WhiI	1.9805	3.0348
1.22E-35	vnz_12970	penicillin-binding protein	1.8746	1.6578
7.74E-05	vnz_25950	HupS	1.8591	1.4814
7.17E-25	vnz_23255	penicillin-binding protein	1.4519	1.4785
1.04E-17	vnz_15130	penicillin-binding protein	0.8151	0.7076
4.46E-06	vnz_13645	WhiB	0.6179	0.5096

614

615 **Table 1.**

SUPPLEMENTAL FIGURE AND TABLE LEGENDS

Text S1. Supplemental Materials and Methods.

FIG S1. BldC ChIP-seq peaks fall into two classes. BldC binding upstream of some targets generates a broad region of enrichment. For *smeA*, this likely corresponds with the binding of four direct repeats by BldC, observed *in vitro* (Schumacher MA, den Hengst CD, Bush MJ, Le TBK, Tran NT, Chandra G, Zeng W, Travis B, Brennan RG, Buttner MJ. Nat Commun. 2018 9:1139. doi: 10.1038/s41467-018-03576-3). Other BldC ChIP-seq targets e.g. *cdgE, dynAB* display similarly broad regions of enrichment and examination of the nucleotide sequence in these regions likewise reveals four similar and appropriately spaced direct repeats. At other BldC ChIP-seq targets, much narrower regions of enrichment are observed. For *whiI*, this likely corresponds with the binding of just two direct repeats by BldC, observed *in vitro* (Schumacher MA, den Hengst CD, Bush MJ, Le TBK, Tran NT, Chandra G, Zeng W, Travis B, Brennan RG, Buttner MJ. Nat Commun. 2018 9:1139. doi: 10.1038/s41467-018-03576-3). Other BldC ChIP-seq targets e.g. *vnz23255* and *cvnA4-D4* display similarly narrow regions of enrichment and examination of the nucleotide sequence in these regions likewise reveals a pair of similar and appropriately spaced direct repeats. The ChIP-seq panels are identical to those shown in Fig. 5. The AT-rich sequences of the verified (in the case of *whiI* and *smeA*) and candidate direct repeats to which BldC binds are highlighted below in yellow in the 5′-3′ direction.

Table S1A. ChIP-seq data set for *S.venezuelae* BldC.

Only those peaks with significance p < E-04 for at least one of the timepoints are included in the analysis. “Pos” = position in the *S. venezuelae* genome in bases. “lndiff” = the difference between the local normalized (ln) values of the immunoprecipitated wild type samples and Δ*bldC* mutant for each of the time points (lndiff 10hr and lndiff 14hr). “min apv” = minimum

adjusted p-value for the 10 hr and 14 hr timepoints. “Closestgene” = nearest annotated gene relative to the position of significance. “lgene” = the identity of a gene where present on the left of the significant position and in the 5’-3’ direction. “lproduct” = the predicted gene product of the lgene. “ldist” = the distance between the significant position and the predicted start codon of the lgene. “igene” = the identity of a gene where the significant position is found within (“in”) a coding region. “iproduct” = the predicted gene product of igene. “idist” = the distance between the significant position and the predicted start codon of the igene. “rgene” = the identity of a gene where present on the right of the significant position and in the 5’-3’ direction. “rproduct” = the predicted gene product of the rgene. “rdist” = the distance between the significant position and the predicted start codon of the rgene. Where present, for each of lgene, igene and rgene, the relative expression values generated by RNA-seq are listed for each time point (lgene/igene/rgene logFC 10hr and lgene/igene/rgene logFC 14hr). Where the logFC >1, cell values are highlighted in red, where the logFC<-1, cell values are highlighted in yellow.

Table S1B. Complete RNA-seq data for BldC. Shown is the relative gene expression for the Δ*bldC* mutant compared to the wild type at the 10 hr and 14 hr timepoints. For each gene, the log fold change (logFC) and average p-value (apv) is listed at each timepoint. The canonical gene name (if known) and expected gene product are also listed. Where the logFC >1, cell values are highlighted in red, where the logFC<-1, cell values are highlighted in yellow.

Table S1C. BldC represses the transcription of genes during vegetative growth. Listed are BldC ChIP-seq targets that are significantly upregulated (logFC >1) in the absence of *bldC* during vegetative growth at either the 10 hr or 14 hr timepoints, as determined by RNAseq. Ordered by logFC at 10hr and then by logFC at 14hr. For each ChIP-seq target, the position,

minimum adjusted p-value (min apv), the gene, expected product and distance to the predicted start codon (dist) is also listed. Where the logFC >1, cell values are highlighted in red, where the logFC<-1, cell values are highlighted in yellow.

Table S1D. Selected RNA-seq data for the *dcw* cluster (A), the conservons (B) and genes involved in aerial mycelium formation (C) For each gene, the gene product and log fold change (logFC 10 hr and logFC 14 hr) is listed. Where the logFC >1, cell values are highlighted in red, where the logFC<-1, cell values are highlighted in yellow.

Table S1E. BldC activates the transcription of genes during vegetative growth. Listed are BldC ChIP-seq targets that are significantly downregulated (logFC <-1) in the absence of *bldC* during vegetative growth, as determined by RNAseq. Ordered by logFC at 10hr and then by logFC at 14hr. For each ChIP-seq target, the position, minimum adjusted p-value (min apv), the gene, expected product and distance to the predicted start codon (dist) is also listed.

Table S2. Analysis of BldC ChIP-seq "peaks". For each maximum significant position (Max Sig Pos) or ChIP-seq "peak" (as listed in Table S1A), the genomic positions of the left-most (Pos L) and right-most (Pos R) significant positions are recorded as well as the distance between these positions (Width) at both the 10 hr and 14 hr timepoints. "FASTA" = nucleotide sequences between pos L and pos R. "Nearest Gene" = closest gene to the maximum significant position. "Class" = the class of BldC enrichment observed upon manual inspection of the ChIP-seq peak. BldC binding generates either a narrow or broad region of enrichment. BldC targets with broad regions of enrichment generally correlate to "peak"

690 widths >300bp and examination of the nucleotide sequences reveals multiple AT-rich
691 sequences that would support BldC-multimerisation similar to that observed in the *smeA*-
692 BldC structure (Schumacher MA, den Hengst CD, Bush MJ, Le TBK, Tran NT, Chandra G,
693 Zeng W, Travis B, Brennan RG, Buttner MJ. Nat Commun. 2018 9:1139. doi:
694 10.1038/s41467-018-03576-3). BldC targets with narrow regions of enrichment generally
695 correlate to "peak" widths <300bp and examination of the nucleotide sequences reveals fewer
696 AT-rich sequences that would support BldC-multimerisation similar to that observed in the
697 *whiI*-BldC structure (Schumacher MA, den Hengst CD, Bush MJ, Le TBK, Tran NT,
698 Chandra G, Zeng W, Travis B, Brennan RG, Buttner MJ. Nat Commun. 2018 9:1139. doi:
699 10.1038/s41467-018-03576-3). Peaks recorded as "Broad*" are broad and >300bp upon
700 manual inspection but their significance based upon the threshold applied in our analysis
701 means that a much narrower region is considered bioinformatically.
702
703 **Table S3.** Strains, Plasmids and Oligonucleotide primers used in this study
704
705 **Movie S1.** Time-lapse microscopy of the wild-type strain carrying the FtsZ-YPet fusion. DIC
706 (A) and YFP-channel (B) movies are at 5 frames per second. The time following the first
707 image is indicated at the bottom left. Images were taken every 30 minutes (DIC 150 ms; YFP
708 100 ms). Movies were assembled in the Fiji software package (http://fiji.sc/Fiji).
709
710 **Movie S2.** Time-lapse microscopy of the *bldC* mutant carrying the FtsZ-YPet fusion. DIC
711 (A) and YFP-channel (B) movies are at 5 frames per second. The time following the first
712 image is indicated at the bottom left. Images were taken every 30 minutes (DIC 150 ms; YFP
713 100 ms). Movies were assembled in the Fiji software package (http://fiji.sc/Fiji).
714

715 **Movie S3.** Time-lapse microscopy of the complemented strain carrying the FtsZ-YPet fusion.
716 DIC (A) and YFP-channel (B) movies are at 5 frames per second. The time following the first
717 image is indicated at the bottom left. Images were taken every 30 minutes (DIC 150 ms; YFP
718 100 ms). Movies were assembled in the Fiji software package (http://fiji.sc/Fiji).
719